Towards the simulation of MHD flow in an entire WCLL blanket mock-up

C. Mistrangelo[a,**], L. Bühler[a], V. Klüber[a], C. Koehly[a]

[a]*Karlsruhe Institute of Technology (KIT), P.O. Box 3640, 76021 Karlsruhe, Germany*

Abstract

In the frame of the EUROfusion breeding blanket research activities, the water cooled lead lithium (WCLL) blanket is considered as reference liquid metal blanket design to be tested in ITER and to be used in a DEMO reactor. For the study of pressure and flow distribution in a WCLL blanket module, magnetohydrodynamic (MHD) phenomena, which result from the motion of the electrically conducting breeder in the intense plasma-confining magnetic field, have to be taken into account. They are due to the induction of electric currents that generate strong electromagnetic forces, which modify the velocity distribution in the blanket compared to hydrodynamic conditions and increase pressure losses. In the WCLL test blanket module (TBM) for ITER a basic geometry, consisting of a rectangular box, representing the breeding zone, is repeated along the poloidal direction. The manifold that distributes and collects the liquid metal features two long poloidal ducts, electrically connected across a common wall. The final goal of the present work is to simulate liquid metal MHD flows in strong magnetic fields in a complete column of a WCLL TBM including poloidal manifolds and 8 breeder units. With this aim, the complexity of the model geometry has been progressively increased and various topologies of computational grids have been considered. First simulations have been performed in a single breeder zone connected with a portion of manifolds in order to test the suitability of the generated grid and the performance of the numerical code for this type of problem. In a second step, the MHD flow at moderate magnetic fields in an entire TBM mock-up has been simulated to get pressure distribution along the manifolds and flow partitioning among breeder units.

Keywords: Liquid metal breeder blanket, water cooled lead lithium (WCLL) blanket, numerical simulations, magnetohydrodynamics (MHD), MHD pressure drop, flow distribution
PACS:

1. Introduction

In the frame of the European design strategy to develop a breeding blanket for a DEMOnstration nuclear fusion reactor, the water cooled lead lithium (WCLL) blanket concept has been selected as one of the driver blanket designs that will be investigated in the International Thermonuclear Experimental Reactor ITER [1]. Reduced activation ferritic-martensitic steel Eurofer is employed as structural material and liquid lead lithium serves as tritium breeder, neutron multiplier and heat carrier.

Liquid metal blanket concepts have feasibility issues that are intrinsically related to the nature of the breeder, which is electrically conducting and interacts with the strong magnetic field that confines the fusion plasma, leading to the induction of electric currents and related electromagnetic Lorentz forces. The magnetohydrodynamic (MHD) phenomena that stem from the interaction of the moving liquid metal with the magnetic field cause peculiar velocity distributions and increased pressure losses compared to hydrodynamic flows in the same geometry.

In the WCLL blanket concept, a certain number of basic geometries, namely rectangular boxes representing the breeding zones, is stacked along the poloidal direction and fixed to the common back plate. In the breeding units the volumetric nuclear heat is removed by cooling pipes immersed in the liquid metal, as visible in Figure 1, where the most recent WCLL TBM design is shown [2].

The strategy used to investigate MHD phenomena in liquid metal blankets combines experiments and numerical simulations. The latter can provide accurate results only if adequate grids are employed to discretize the computational domain, which consists of the fluid region and the solid wall. MHD flows are characterized by the development of boundary layers along solid surfaces and internal layers in the fluid at electrical or geometrical discontinuities of the wall. The thickness of the layers reduces by increasing the intensity of the applied magnetic field and their resolution requires a minimum number of grid points [3]. In order to limit the total number of mesh nodes, non-uniform grids are employed that are coarser in the core regions and refined towards the walls. MHD boundary layers are best resolved by using prism cells. Structured grids, i.e. orthogonal and with non-skewed cells, lead usually to better numerical performance, but their poor adaptability to arbitrary geometries can be considered as their ma-

*Corresponding author
**Principal corresponding author
Email address: chiara.mistrangelo@kit.edu (C. Mistrangelo)

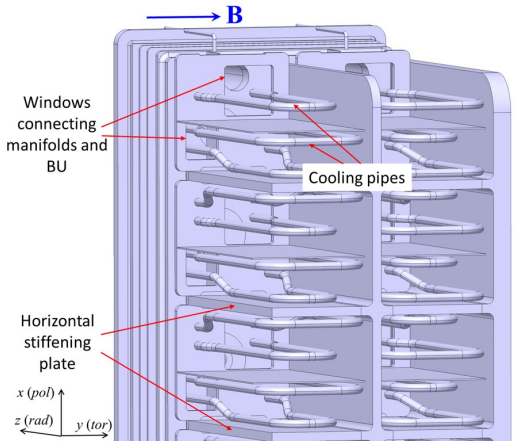

Figure 1: Design of the WCLL TBM for ITER [2]. View on the cooling pipes in the breeding zones.

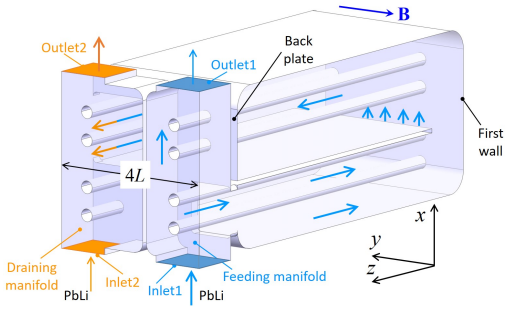

Figure 2: Model geometry for test simulations consisting of a single breeding zone connected to a part of the manifold. Here only the fluid domain is visualized.

jor drawback. For the analysis of MHD flows in complex geometries, such as those typical for fusion applications, hybrid unstructured meshes seem more suitable to meet the resolution requirements without excessive computational costs. However, the skewness of cells in unstructured meshes makes difficult the numerical approximation of gradients of flow variables. A common procedure to overcome this problem foresees the use of discretization schemes with a non-orthogonality correction.

Moreover, the mesh generation procedure should allow an automatic meshing of a CAD model and permit effective control of local refinement in shear layers and regions of interest. Since the presence of an intense magnetic field together with the use of non-orthogonal meshes can lead to the amplification of initially small numerical errors and their propagation along grid lines and magnetic field lines, optimization of grid generation and improvement of numerical schemes are mandatory for fusion applications with strong magnetic fields and arbitrary geometries.

In the present work we discuss numerical results obtained by using an hybrid mesh to study MHD flow in a simplified model geometry consisting of a single breeder unit connected to a portion of the manifolds (Figure 2). This case is used to test the applied mesh generation methods and the performance of the numerical solver that uses a non-orthogonal correction when regions with an unstructured grid are present. The complexity of the model is then increased and the experience gained with the previous computational exercise is applied to the study of MHD flow in an entire WCLL TBM mock-up used for experiments in the MEKKA laboratory at KIT [4].

It should be also mentioned that MHD flows in WCLL blankets differ from those in other design concepts since water cooled pipes are immersed in the liquid metal that slowly circulates in the breeding units. Their presence obstructs the breeder circulation and causes the development through the entire fluid domain of internal shear layers tangent to the pipes and parallel to magnetic field lines. Another important effect that has to be taken into account is the electromagnetic coupling of neighboring domains via leakage currents that are exchanged across the common wall separating the two poloidal ducts, which form the manifold, and across the stiffening plates.

2. Problem configuration and governing equations

2.1. Model geometry

In order to test the performance of the code when the computational domain is discretized via an hybrid mesh, a model geometry has been selected, as shown in Figure 2, featuring a breeder unit with dummy cooling pipes and connected to a portion of the two poloidal channels of the manifold. A uniform magnetic field is applied in toroidal direction. Since the final aim is to simulate MHD flow in an experimental mock-up and to compare numerical and experimental results, simulations have been carried out considering the sodium potassium alloy NaK as model fluid, as employed for the experiments.

After evaluating the quality of the mesh and the performance of the code by using the simplified geometry, simulations have been carried out to predict the MHD flow in the complete experimental mock-up when exposed to moderate magnetic fields. Figure 3 displays the design of the test-section with the principle sketch of the liquid metal path. The feeding manifold of the mock-up is supplied with NaK by a circular pipe, the model fluid distributes among the breeder zones (blue line) passing through windows in the back plate, circulates in radial direction to approach the first wall, turns in poloidal direction around the stiffening plate before flowing radially towards the collecting windows and into the draining manifold (orange line). A detailed description of the experimental test-section, installation and instrumentation can be found in [4].

2.2. Numerical set-up

We consider the flow of an electrically conducting fluid, such as a liquid metal, exposed to an externally applied

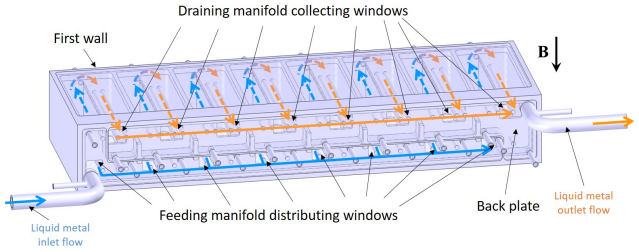

Figure 3: Experimental mock-up with schematic liquid metal path. The body of the test-section has a poloidal size of 668.4 mm, a radial dimension of 222.6 mm and a toroidal one of 102 mm.

uniform magnetic field $\mathbf{B} = B\hat{\mathbf{y}}$. The viscous, incompressible flow is governed by equations for balance of momentum, conservation of mass, and currents are calculated by Ohm's law

$$\rho\left(\frac{\partial}{\partial t} + \mathbf{v}\cdot\nabla\right)\mathbf{v} = -\nabla p + \rho\nu\nabla^2\mathbf{v} + \mathbf{j}\times\mathbf{B}, \qquad (1)$$

$$\nabla\cdot\mathbf{v} = 0,\ \mathbf{j} = \sigma(-\nabla\phi + \mathbf{v}\times\mathbf{B}). \qquad (2)$$

Here $\mathbf{v}$, $\mathbf{j}$, $\mathbf{B}$ and ϕ indicate velocity, current density, applied magnetic flux density, and electric potential. The physical properties of the fluid, density ρ, kinematic viscosity ν, and electric conductivity σ, are assumed to be constant and taken for the experimental model fluid sodium potassium (NaK) at 30°C [5]. The electric potential ϕ is determined by a Poisson equation obtained by combining Ohm's law (2) with the condition for charge conservation $\nabla\cdot\mathbf{j} = 0$:

$$\nabla^2\phi = \nabla\cdot(\mathbf{v}\times\mathbf{B}). \qquad (3)$$

In the wall this equation reduces to $\nabla^2\phi_w = 0$.

As kinematic boundary conditions at the walls the no-slip condition, $\mathbf{v} = 0$, is applied. The external surface of the walls are electrically insulating, $\partial\phi_w/\partial n = 0$, and at the fluid-wall interface the solution in the fluid is coupled to the one in the wall by imposing continuity of potential and normal component of current density.

The flow is characterized by two dimensionless parameters the Hartmann number, Ha and the Reynolds number, Re:

$$Ha = BL\sqrt{\frac{\sigma}{\rho\nu}},\ Re = \frac{u_0 L}{\nu}. \qquad (4)$$

The former one gives a non-dimensional measure for the strength B of the imposed magnetic field and its square describes the relative importance of electromagnetic and viscous forces. The Reynolds number indicates the ratio of inertia to viscous forces and can be also expressed as $Re = Ha^2/N$, where $N = \sigma LB^2/(\rho u_0)$ is the interaction parameter. The quantity L, known as Hartmann length, is a characteristic size of the geometry, taken as a quarter of the dimension of the breeder unit measured along magnetic field direction (see Figure 2) and u_0 is a typical velocity in the problem.

The equations governing the problem have been implemented in the open source code OpenFOAM. A cell-centered finite volume method is used to discretize the equations. A segregated solver is employed and for the coupling between pressure and velocity the Pressure Implicit with Splitting of Operators (PISO) algorithm is used. The Lorentz force is treated explicitly and defined at cell-centers. Centroid currents required for determination of the electromagnetic force are obtained by interpolation from face current fluxes by using the identity $\mathbf{j} = \nabla\cdot(\mathbf{jr})$, where $\mathbf{r}$ is the distance vector [6, 7], in order to avoid spurious contributions to the Lorentz force due to discretisation errors. The standard Gaussian finite volume integration is employed for discretisation of convective terms, together with a second order skewness-corrected interpolation scheme required when using non-orthogonal meshes.

3. Numerical results

As already mentioned, accurate simulations of MHD flows is possible only with proper resolution of boundary and internal layers. In the problem under study internal layers aligned with the magnetic field develop both tangent to the pipes and at the windows in the back plate where the liquid metal expands and contracts moving along field lines to enter and exit the breeder zones, respectively. Boundary layers that form at walls where $\mathbf{B}$ has a perpendicular component are called Hartmann layers and those at walls parallel to the magnetic field are referred to as side or parallel layers. The thickness of the layers reduces with increasing strength of the magnetic field: for the Hartmann layers is $\delta_{Ha} \sim O(Ha^{-1})$, while for the side layers $\delta_S \sim O(Ha^{-1/2})$. Benchmark activities related to the study of fully developed MHD flows aiming at validating the employed numerical code showed that accurate prediction of velocity distribution and pressure gradient in a channel needs at least 7 points in the Hartmann layers and 20 nodes in the side layers [3].

For the present investigation, in order to limit the total number of computational cells while keeping a suitable resolution of boundary and internal layers, a hybrid mesh with local refinement has been generated. It is characterized by interface-aligned prism layers near the walls and along the cooling pipes, a regular core grid and unstructured regions to join the two mesh portions. Three dimensional simulations have been performed on the supercomputers JFRS - 1 at IFERC - CSC and on Marconi - CINECA by using 140 CPUs for simulations of MHD flows in a single breeder unit (Figure 2) and 550 CPUs for the complete mock-up (Figure 3).

3.1. MHD flow in a simplified test geometry

With the purpose of testing the automatic mesh generation procedure and to verify the performance of the solver

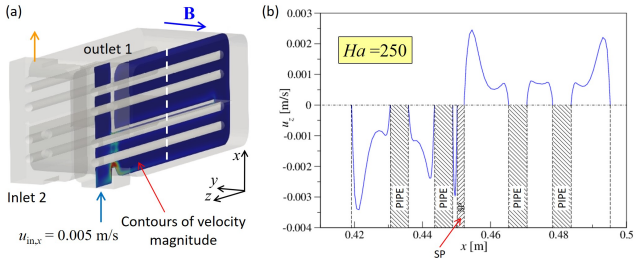

Figure 4: Flow in the model geometry (single breeder unit) at $Ha = 250$ and inlet velocity $\mathbf{u}_{in} = (0.005, 0, 0)$. (a) Contours of velocity magnitude on a xz plane. (b) Transverse velocity component u_z along the white dashed line in (a).

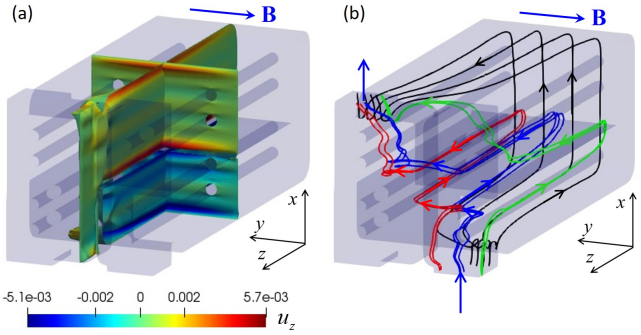

Figure 5: Flow in the model geometry at $Ha = 250$ and inlet velocity $\mathbf{u}_{in} = (0.005, 0, 0)$[m/s]. Contours of radial velocity u_z are plotted on two planes showing the development of internal and parallel layers (a). Streamlines seeded at the entrance of the geometry showing the main liquid metal flow paths (b).

with this type of grid, simulations have been carried out to predict the MHD flow in a single breeder zone fed and drained by a part of the manifold. Results are presented for $Ha = 250$ and an inlet velocity $u_{in,x} = 0.005$m/s.

The used meshing workflow creates a high quality 3D hex-dominant mesh with polyhedral in transition regions between cells of different size. Boundary layers are resolved by thin prism layers. It is assumed that *outlet*1 and *inlet*2 are closed (Figure 2). Different types of mesh and solution algorithms have been tested to avoid numerical errors and local spurious perturbations in the solution. Critical regions for mesh resolution have been identified; in addition to boundary and internal layers, there are also narrow passages between pipes and horizontal plates that require careful treatment. This can be seen in Figure 4b where the transverse component u_z of the velocity is plotted along the white dashed line in Figure 4a as a function of the poloidal coordinate x. Between a pipe and the stiffening plate (SP) there is a narrow gap with large velocity. For this moderate magnetic field (0.22T), side layers are relatively thick and therefore they almost merge with internal layers that develop tangentially to the cooling pipes, while by increasing the Hartmann number, they become thinner and a more evident separation between cores and layers can be observed. A uniform core, as expected in duct flow, is not present, since the liquid metal has to circulate around the pipes and internal layers propagate along magnetic field lines crossing the entire breeder unit.

The main features of the MHD flow in the breeder zone and in the manifold portion are highlighted in Figure 5. Here contours of radial velocity u_z are depicted on two planes (a) and a representative set of velocity streamlines that capture the flow behavior are obtained by placing seed points in the center of *inlet*1 (b). The highest velocity is localized in the boundary layers at walls aligned with the magnetic field, especially along the external walls and the stiffening plate (SP). Blue and red streamlines show how the fluid moves upwards, expands from the manifold in the breeding zone by following a path in magnetic field direction, before flowing in radial direction. At the first wall the liquid metal turns in poloidal direction and moves back towards the draining manifold. At the back plate the fluid flows parallel to the magnetic field in a layer and enters the collecting manifold through a square window. The green streamlines are seeded in the manifold very close to the Hartmann layers where they remain till reaching the back plate along which they flow before entering the draining manifold. The black streamlines originate from seed points near the back plate. These paths move in the breeding zone and proceed in the side layers all around the breeder unit. The presence of the pipes forces the liquid metal to flow around them, causing locally the occurrence of curves in the streamlines (see green, blue and red lines).

Simulations of MHD flows in a single breeder unit have been carried out for two inlet velocities, $u_{in,x} = 0.005$m/s and 0.01m/s, various grids, and by applying different tolerances for the residuals, solution algorithms and under-relaxation factors to improve the numerical stability of the computation. By evaluating the results of this study, a mesh has been selected as well as optimized solution control parameters for the simulation of MHD flow in the entire mock-up that will be used for experiments (Figure 3). Preconditioned conjugate gradient (PCG) and its variants such as bi-conjugate (BiCG) and stabilized BiCG are used for the solution of pressure, velocity and potential equations, respectively.

3.2. MHD flow in an experimental mock-up

In the following first results for the liquid metal MHD flow in an entire experimental mock-up of a WCLL TBM, shown in Figure 3, are described for a uniform magnetic field, $Ha = 150$, and an inlet velocity $u_{in,x} = 0.01$m/s. In Figure 6a velocity streamlines are plotted in the mock-up, visualizing the liquid metal path both in the manifold ducts and in the breeder units. The fluid passes from the inlet pipe into the manifold and a part of it enters the window connecting the feeding manifold with BU1 (see red streamlines). The liquid metal then flows along the stiffening plate, it returns towards the back plate to be collected by the second poloidal duct. The remaining liquid metal should distribute along the manifold among the

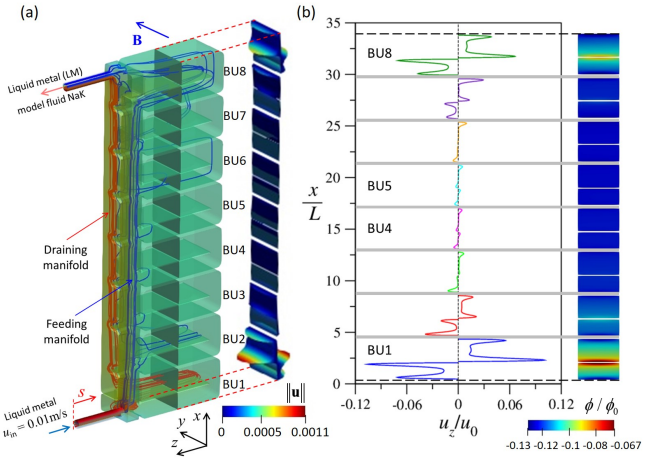

Figure 6: Flow in the experimental mock-up of a WCLL TBM at $Ha = 150$ and inlet velocity $\mathbf{u}_{in} = (0.01, 0, 0)$[m/s]. Velocity streamlines and 3D velocity contours in the middle xy plane of the geometry (a). Velocity profile in the center of the module and electric potential distribution on the same xy plane (b).

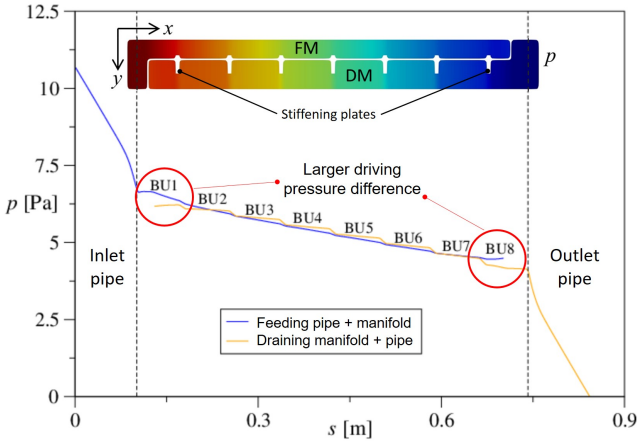

Figure 7: Pressure along pipes, feeding (FM) and draining (DM) manifolds. Coordinate s starts at the inlet pipe (see Figure 6a). In the subplot contours of pressure are shown on a xy plane in the manifold. Stiffening plates are visible that reduce locally the cross-section of the liquid metal paths in particular along the draining manifold DM.

other seven BUs, but the largest portion flows directly to BU8. Profiles of radial velocity u_z in the BUs are displayed both as 3D contours on the xy plane in the middle of the mock-up (Figure 6a) and as 2D graph along the poloidal line in the center of the module (Figure 6b). Here the velocity has been scaled by the inlet velocity, $u_0 = u_{in}$. As expected in electrically conducting channels, the velocity distribution is characterized by side layer jets along walls parallel to the magnetic field. It can be observed that the flow rate in BU1 and BU8 is much larger than the one in the other breeding zones. In BU4 and BU5 there is almost no flow. The velocity distribution resembles the one obtained by numerical calculations for the MHD flow in a helium cooled lead lithium (HCLL) blanket mock-up, which were confirmed by experimental data for electric potential on the Hartmann wall [8]. Contours of electric potential on the same xy plane, shown in Figure 6b, exhibit analogous larger values in the first and last breeding zones.

The reason behind the significant flow imbalance is the geometry of the manifold where the cross-sections of the two poloidal ducts remain on average constant when the liquid metal moves in poloidal direction. On the other hand, the flow rate in the feeding and draining manifolds reduces and increases, respectively. For a better performance of the TBM with more uniform flow partitioning among all BUs, the manifold design should be modified so that the cross-section of the ducts adapts to the changing flow rates along the poloidal liquid metal path. The cause of the non uniform flow partitioning among BUs had been already identified in the studies of MHD flows in the HCLL blanket.

These non homogeneous characteristics of the flow in the WCLL blanket mock-up is evidenced by the pressure distributions along the manifolds that are plotted in Figure 7. The steps in the pressure profiles are due to the periodic occurrence of expansions and contractions along the liquid metal flow path in the manifolds. These constrictions are caused by the penetration of the stiffening plates in the poloidal ducts (see xy plane in the subplot in Figure 7). The local pressure jumps are higher in the draining manifold since there the reduction of the cross-section is more significant than in the feeding one. The differences of pressure in feeding and draining manifolds constitute the pressure heads between entrance and exit of the BUs and they are obviously not the same for all BUs. At both module ends, highlighted by red circles, there are larger driving pressure differences causing stronger flow through BU1 and BU8 compared to the ones in the other BUs.

4. Conclusions

The investigation of MHD effects in liquid metal flows is required to predict velocity distribution and pressure losses in blankets for fusion reactors. A synergy between experiments and numerical simulations has to be exploited to get a complete understanding of these phenomena and to draw conclusions about their influence on the performance of liquid metal blankets. Apart from few specific studies [9][10], direct numerical simulations have still limitations in their applicability. When considering entire blanket modules, the maximum Hartmann number that can be reached is often limited or the accuracy of the results cannot be ensured due to the extremely large number of grid points required to properly resolve all boundary and internal layers that develop in such complex geometries. A method to make progresses is to employ hybrid meshes in which topologically different grids are combined to satisfy the local computational requirements. Best performances in the simulation of MHD flows at large Hart-

mann numbers have been obtained by using hex-dominant meshes with prism elements in boundary regions. However, the dimension of cells for the resolution of layers is usually much smaller than the one needed in core regions. In order to minimize the number of grid points, transitional unstructured meshes are employed between structured zones, which have very different cell size. The automatic generation of a suitable MHD mesh involves a significant number of actions for a local optimization and careful treatment of boundary and internal layers. These critical regions form along all walls, at expansions and contractions and near sharp bends present along the liquid metal flow path. In the present study we investigated the performance of the applied code when using an hybrid mesh and adequate numerical schemes to minimize possible errors due to skewness of the cells. As a test case the MHD flow in a single breeder unit connected to manifold ducts has been selected. Simulations have been performed for $50 \leqslant Ha \leqslant 1000$ and two inlet velocities $u_{in} = 0.005, 0.01\text{m/s}$. It has been confirmed that the use of unstructured meshes for the simulation of MHD flows, especially at moderate and large Ha, requires non-orthogonal corrections when approximating the gradients of variables at cell faces.

First simulations of MHD flows in an entire experimental mock-up of a WCLL TBM yield results that are consistent with previous investigations. It has been found that the present manifold design leads to non-uniform flow partitioning among the 8 BUs. The first and last breeding zones (BU1 and BU8) exchange much of the flux between both manifolds, whereas there is almost no flow in the center of the module in BUs 3-6. Therefore, an update of the manifold geometry is strongly recommended during future design activities.

The present paper provides first insight in the physical behavior of MHD flows in an entire WCLL TBM mock-up. In future numerical simulations, the mesh will be refined and the number of CPUs increased to predict MHD flows under stronger magnetic fields to reach fusion relevant operating conditions. A comparison with upcoming experimental data will allow to further validate the code and the numerical procedures.

Acknowledgment

This work has been carried out within the framework of the EUROfusion Consortium, funded by the European Union via the Euratom Research and Training Programme (Grant Agreement No 101052200 — EUROfusion). Views and opinions expressed are however those of the author(s) only and do not necessarily reflect those of the European Union or the European Commission. Neither the European Union nor the European Commission can be held responsible for them. This work was carried out (partially) using supercomputer resources provided under the EU-JA Broader Approach collaboration in the Computational Simulation Centre of International Fusion Energy Research Centre (IFERC-CSC).

References

[1] G. Federici, L. Boccaccini, F. Cismondi, M. Gasparotto, Y. Poitevin, I. Ricapito, An overview of the EU breeding blanket design strategy as an integral part of the DEMO design effort, Fusion Engineering and Design 141 (2019) 30 – 42. doi:https://doi.org/10.1016/j.fusengdes.2019.01.141.

[2] J. Aubert, G. Aiello, D. Alonso, T. Batal, R. Boullon, S. Burles, B. Cantone, F. Cismondi, A. Del Nevo, L. Maqueda, A. Morin, E. Rodríguez, F. Rueda, M. Soldaini, J. Vallory, Design and preliminary analyses of the new water cooled lithium lead tbm for iter, Fusion Engineering and Design 160 (2020) 111921. doi:https://doi.org/10.1016/j.fusengdes.2020.111921.

[3] S. Smolentsev, S. Badia, R. Bhattacharyay, L. Bühler, L. Chen, Q. Huang, H.-G. Jin, D. Krasnov, D.-W. Lee, E. Mas de les Valls, C. Mistrangelo, R. Munipalli, M.-J. Ni, D. Pashkevich, A. Patel, G. Pulugundla, P. Satyamurthy, A. Snegirev, V. Sviridov, P. Swain, T. Zhou, O. Zikanov, An approach to verification and validation of MHD codes for fusion applications, Fusion Engineering and Design 100 (2015) 65–72. doi:http://dx.doi.org/10.1016/j.fusengdes.2014.04.049.

[4] C. Koehly, L. Bühler, Design of a scaled mock-up of the WCLL TBM for mhd experiments in liquid metal manifolds and breeder units, in: Proceedings of the 32th Symposium on Fusion Technology SOFT, Dubrovnik, Croatia, September 18-23, 2022, 2022.

[5] O. J. Foust, Sodium - NaK Engineering Handbook, Gordon and Breach Science Publishers, New York, London, Paris, 1972.

[6] M.-J. Ni, R. Munipalli, N. B. Morley, P. Huang, M. A. Abdou, A current density conservative scheme for incompressible MHD flows at a low magnetic Reynolds number. Part I: On a rectangular collocated grid system, Journal of Computational Physics 227 (1) (2007) 174–204.

[7] M.-J. Ni, R. Munipalli, P. Huang, N. B. Morley, M. A. Abdou, A current density conservative scheme for incompressible MHD flows at a low magnetic Reynolds number. Part II: On an arbitrary collocated mesh, Journal of Computational Physics 227 (1) (2007) 205–228.

[8] C. Mistrangelo, L. Bühler, Determination of multichannel MHD velocity profiles from wall-potential measurements and numerical simulations, Fusion Engineering and Design 130 (2018) 137–141. doi:10.1016/j.fusengdes.2018.03.041.

[9] Y. Yan, A. Ying, M. Abdou, Numerical study of magneto-convection flows in a complex prototypical liquid-metal fusion blanket geometry, Fusion Engineering and Design 159 (2020) 111688. doi:https://doi.org/10.1016/j.fusengdes.2020.111688.

[10] L. Chen, S. Smolentsev, M.-J. Ni, Toward full simulations for a liquid metal blanket: MHD flow computations for a PbLi blanket prototype at $Ha \sim 10^4$, Nuclear Fusion 60 (7) (2020) 076003. doi:10.1088/1741-4326/ab8b30.